

Spatial and temporal variations in vector fields

C. Macías-Romero,* M. R. Foreman, and P. Török

Blackett Laboratory, Imperial College London, London SW7 2BZ, UK

[*cm1105@ic.ac.uk](mailto:cm1105@ic.ac.uk)

Abstract: We introduce a new metric to characterise spatial variations occurring in a time varying vector field, and we derive a rotationally invariant formula that quantifies temporal fluctuations within a consistent framework. So as to highlight the physics behind these metrics, both are derived from a well-known experiment in polarimetry. The derivation yields a set of expressions in a two-dimensional space, which is subsequently expanded to n -dimensions for special cases. The resulting expressions of the temporal and spatial metrics are incorporated into the electromagnetic theory of coherence and polarisation. Examples are given in the context of single molecule detection when measuring asymmetrically and radially polarised beams.

© 2011 Optical Society of America

OCIS codes: (260.2130) Ellipsometry and polarimetry; (030.0030) Coherence and statistical optics; (110.5405) Polarimetric imaging.

References and links

1. J. Ellis and A. Dogariu, "Optical polarimetry of random fields," *Phys. Rev. Lett.* **95**(20), 203905 (2004).
2. A. F. Abouraddy and K. C. Toussaint, "Three-dimensional polarization control in microscopy," *Phys. Rev. Lett.* **96**(15), 153901 (2006).
3. K. Serrels, E. Ramsay, R. Warburton, and D. Reid, "Nanoscale optical microscopy in the vectorial focusing regime," *Nature Phot.* **2**(5), 311–314 (2008).
4. T. Ha, T. Enderle, D. S. Chemla, P. R. Selvin, and S. Weiss, "Single Molecule Dynamics Studied by Polarization Modulation," *Phys. Rev. Lett.* **77**(19), 3979–3982 (1996).
5. E. Wolf, "Optics in terms of observable quantities," *Il Nuovo Cimento* **12**(6), 884–888 (1954).
6. P. Munro and P. Török, "Properties of high-numerical-aperture Müller-matrix polarimeters," *Opt. Lett.* **33**, 2428–2430 (2008).
7. T. Shirai and E. Wolf, "Correlations between intensity fluctuations in stochastic electromagnetic beams of any state of coherence and polarization," *Opt. Commun.* **272**(2), 289–292 (2007).
8. H. C. Jacks and O. Korotkova, "Intensity–intensity fluctuations of stochastic fields produced upon weak scattering," *J. Opt. Soc. Am. A* **28**(6), 1139–1144 (2011).
9. E. Wolf, "Coherence properties of partially polarized electromagnetic radiation," *Il Nuovo Cimento* **13**(6), 1165–1181 (1959).
10. T. Setälä, A. Shevchenko, M. Kaivola, and A. Friberg, "Degree of polarization for optical near fields," *Phys. Rev. E* **66**(1), 16615 (2002).
11. U. Fano, "A Stokes-Parameter Technique for the Treatment of Polarization in Quantum Mechanics," *Phys. Rev.* **93**(1), 121–123 (1954).
12. M. Neil, T. Wilson, and R. Juskaitis, "A wavefront generator for complex pupil function synthesis and point spread function engineering," *J. Microscopy* **197**, 219–223 (2000).
13. J. Gil, "Polarimetric characterization of light and media," *Europ. Phys. J. App. Phys.* **40**(1), 1–47 (2007).
14. J. Ellis, A. Dogariu, S. Ponomarenko, and E. Wolf, "Degree of polarization of statistically stationary electromagnetic fields," *Opt. Commun.* **248**(4–6), 333–337 (2005).
15. R. M. A. Azzam and N. M. Bashara, *Ellipsometry and Polarized Light* (North-Holland, Amsterdam, 1977).
16. J. Movilla, G. Piquero, R. Martínez-Herrero, and P. Mejías, "Parametric characterization of non-uniformly polarized beams," *Opt. Commun.* **149**(4–6), 230–234 (1998).

17. J. Ellis and A. Dogariu, "Complex degree of mutual polarization," *Opt. Lett.* **29**(6), 536–538 (2004).
18. H. Moya-Cessa, J. R. Moya-Cessa, J. Landgrave, A. Martinez-Niconoff, G. and Perez-Leija, and A. T. Friberg, "Degree of polarization and quantum-mechanical purity," *J. Europ. Opt. Soc. Rap. Public.* **3**(5), 08014 (2008).
19. P. Török, P. Higdon, and T. Wilson, "On the general properties of polarised light conventional and confocal microscopes," *Opt. Comm.* **148**(4–6), 300–315 (1998).

1. Introduction

The study of polarisation of light has recently attracted considerable interest due, for example, to applications in polarisation imaging [1], focal-volume engineering [2], high resolution optical microscopy [3], and molecular dynamics [4]. In particular, polarisation sensitive imaging has shown a growth in popularity in areas such as biology and medicine. It is well known, for example, that cancerous and healthy cells affect the polarisation of the light differently. However, the major issue in polarisation applications is that the amount of non-redundant information obtained is such that the data analysis usually requires highly skilled interpreters.

A common mistake in polarisation sensitive measurements is the interpretation of spatial variations in the polarisation as depolarisation, i.e. temporal random fluctuations [5]. It is not true for example that a field is depolarised when passing through a temporally-static scattering material or a high numerical aperture (NA) lens. The field in both examples is actually inhomogeneously polarised in the spatial sense. Given that point-detectors are theoretical entities, the mistake arises when the spatial extent of the polarisation variations happen over smaller scales than the detection domain of the optical system, which could for example be a single CCD pixel. A polarisation sensitive imaging system averages over the spatial extent of the detector resulting in a single aggregate polarisation reading [6]. It is for this reason that a clear difference between spatial variations and temporal fluctuations must be made.

In this paper we introduce the degree of spatial polarisation (DOSP) to account for spatial variations in the polarisation regardless of temporal fluctuations. The resulting formula is incorporated into the theory of coherence and polarisation; fluctuations in the irradiance as a result of spatial polarisation variations are discussed elsewhere [7, 8]. We also derive the degree of temporal polarisation (DOTP), in a notation consistent with that of the DOSP, to account for temporal fluctuations regardless of spatial variations. The resulting expression of the DOTP is shown to be invariant to rotations of the co-ordinate system used. The DOTP is shown to reduce to the current definition of the two- [9] and three-dimensional [10] degree of polarisation for special cases. Note that the results given here have both quantum and classical applications given that the final expressions are written in terms of the polarisation matrix [11, 5].

The principles described above are explored using the null-polarimeter experiment shown in Fig. 1, which can be used to measure the degree of temporal polarisation. In this experiment a field, which is possibly fluctuating randomly in time and containing a transverse polarisation distribution, passes through a spatially inhomogeneous analyser to then be incident on a CCD. In the case of a collimated beam being analysed such a device can for example be realised by a vectorial beam shaping unit [12] and a Glan-Thompson polariser. As seen next, the DOTP and DOSP can be derived from the irradiance distribution on the CCD resulting from different settings of the analyser. General notation is introduced next followed by the derivation of the DOSP in section 3 and the DOTP in section 4. A series of remarks and examples are given in section 5 and 6, respectively.

2. General notation

The derivation of the DOSP will follow from the correlation between the polarised part of different patches in the field, and the DOTP will be derived from finding the amount of unpolarised light in respect to the polarised part. We thus proceed to write the mathematical expres-

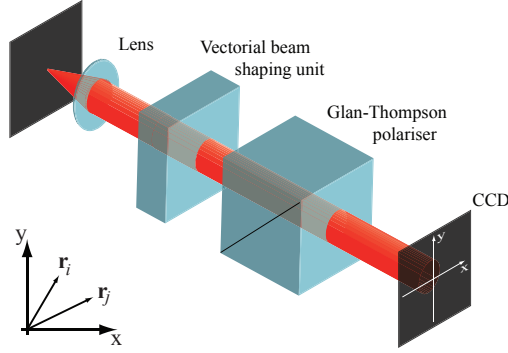


Fig. 1. Null-polarimeter experiment.

sion of the null-polarimeter experiment in terms of the polarisation matrix and eigenspaces. The use of the eigenspaces allows one to control the settings of the analyser. Given that depolarisation is a linear effect [13] we may represent the field incident on the analyser $\Gamma_j = \Gamma(\mathbf{r}_j, \mathbf{r}_j, 0) = \langle \vec{\mathbf{E}}(\mathbf{r}_j, t) \otimes \vec{\mathbf{E}}^\dagger(\mathbf{r}_j, t + \tau) \rangle$ for $\tau = 0$, with \otimes representing the Kronecker product and $\langle \dots \rangle$ denoting time average (wide sense stationary random processes are assumed), as a sum of two matrices:

$$\Gamma_j = \Gamma_j^p + \Gamma_j^u, \quad (1)$$

where $\Gamma_j^u = \alpha_j \mathbf{I}$ represents the temporally unpolarised portion of the field, and Γ_j^p is a matrix of rank one representing the part of the field that it is totally temporally polarised, i.e. a pure state. Here $\mathbf{r}_j = (x_j, y_j, z_j)$ is a position vector denoting a point in the field, and α_j is the magnitude of the temporally unpolarised part of the field at that point.

The distribution of the irradiance detected by the CCD is described by [14, 15]

$$\text{Tr} [\tilde{\mathbf{G}}_i \Gamma_j \tilde{\mathbf{G}}_i^\dagger] = \text{Tr} [\tilde{\mathbf{G}}_i \Gamma_j^p \tilde{\mathbf{G}}_i^\dagger] + \text{Tr} [\tilde{\mathbf{G}}_i \Gamma_j^u \tilde{\mathbf{G}}_i^\dagger], \quad (2)$$

where $\tilde{\mathbf{G}}_i = \tilde{\mathbf{G}}(\mathbf{r}_i)$ denotes a matrix describing the transmission of a field through the system, i.e. polarisation analyser, and Tr is the trace operator. Here $\mathbf{r}_i = (x_i, y_i, z_i)$ is a position vector denoting a point in the system. The \sim notation signifies a dimensionless quantity throughout this paper. The transmission can thus be nulled by matching the eigenvectors of $\tilde{\mathbf{G}}_i$ to those of Γ_j^p and choosing the eigenvalues of the former such that zero transmittance occurs. Γ_j^p is hence written as

$$\Gamma_j^p = \tilde{\mathbf{X}}_j \Lambda_j^p \tilde{\mathbf{X}}_j^\dagger,$$

where $\tilde{\mathbf{X}}_j$ are the eigenvectors associated with the j^{th} patch of the field, and Λ_j^p is a diagonal matrix whose elements are the eigenvalues of Γ_j^p . The spatially inhomogeneous analyser is then defined as

$$\tilde{\mathbf{G}}_i = \tilde{\mathbf{X}}_i \tilde{\Phi}_i \tilde{\mathbf{X}}_i^\dagger, \quad (3)$$

where $\tilde{\mathbf{X}}_i$ are the eigenvectors associated with the i^{th} patch of the analyser and $\tilde{\Phi}_i$ is a diagonal matrix whose elements are the eigenvalues of $\tilde{\mathbf{G}}_i$. It then follows that Γ_j^p can be extinguished for $i = j$ if the eigenvalues of $\tilde{\mathbf{G}}_i$ are defined as

$$\tilde{\Phi}_i = \sqrt{\tilde{\lambda}_i^p \mathbf{I} - \tilde{\Lambda}_i^p}, \quad (4)$$

where $\tilde{\lambda}_i^p = \lambda_i^p / \text{Tr}[\Gamma_i^p]$. Here λ_i^p is the non-zero eigenvalue of Γ_i^p and $\tilde{\Lambda}_i^p$ is a diagonal matrix whose only non-zero element is $\tilde{\lambda}_i^p$. Since $\tilde{\mathbf{G}}$ is by definition dimensionless, it is necessary for $\tilde{\Phi}_i$ and $\tilde{\mathbf{X}}_i$, to also be dimensionless.

Notice that for practical purposes, one would assume that the field represented by Γ_j possesses a number of homogeneously polarised patches indexed by j , and the polarisation analyser represented by $\tilde{\mathbf{G}}_i$ possesses a number of homogeneously analysing patches indexed by i .

3. Degree of spatial polarisation

The degree of spatial polarisation is derived by finding the correlation between the polarised part of different patches in the field. For this Eqs. (3) and (4) are substituted into the polarised part of the field:

$$I^p(\mathbf{r}_i, \mathbf{r}_j) = I_{(i,j)}^p = \text{Tr}[\tilde{\mathbf{G}}_i \Gamma_j^p \tilde{\mathbf{G}}_i^\dagger], \quad (5)$$

to yield

$$I_{(i,j)}^p = \text{Tr}[\tilde{\Gamma}_i^p] \text{Tr}[\Gamma_j^p] - \text{Tr}[\Gamma_j^p \tilde{\Gamma}_i^p] \quad (6)$$

with the aid of the additive and multiplicative property of the trace, i.e. $\text{Tr}[A+B] = \text{Tr}[A] + \text{Tr}[B]$ and $\text{Tr}[AB] = \text{Tr}[BA]$, respectively. Using Eq. (1), and the following identities (see Eqs. 25 and 26 in the Appendix)

$$\text{Tr}[\Gamma_j] - \lambda_j = \alpha_j(\text{Tr}[\mathbf{I}] - 1), \quad (7)$$

$$\text{Tr}[\tilde{\Lambda}_i \Lambda_j] = \tilde{\lambda}_i \lambda_j + \tilde{\alpha}_i \alpha_j(\text{Tr}[\mathbf{I}] - 1), \quad (8)$$

where $\Lambda_j = \Gamma_j^p + \alpha_j \mathbf{I}$ is a diagonal matrix containing the eigenvalues of Γ_j and $\lambda_j = \lambda_j^p + \alpha_j$, Eq. (6) is rewritten as

$$I_{(i,j)}^p = \text{Tr}[\tilde{\Lambda}_i \Lambda_j] - \text{Tr}[\tilde{\Gamma}_i \Gamma_j]. \quad (9)$$

Equation (9) represents the contribution of the polarised part of the field to the irradiance at the CCD when analysing the field using the polarisation state of a different patch as a reference. What was a point in the system (\mathbf{r}_i) is now a point in the field that is being used as reference. Equation (9) thus expresses the correlation between the polarised part of different points in the field in terms of irradiance. It then follows that normalising Eq. (9) by the total irradiance at each point and subtracting it from unity for convention yields the degree of spatial polarisation:

$$P_{(i,j)}^s \equiv 1 - \frac{\text{Tr}[\Lambda_i \Lambda_j] - \text{Tr}[\Gamma_i \Gamma_j]}{\text{Tr}[\Gamma_i] \text{Tr}[\Gamma_j]}. \quad (10)$$

The derivation considers a nulling experiment that results in minimising the fringe visibility in a Young interferometer. As opposed to the conventional maximisation of the visibility in the fringes. Equation (10) is a measure of the similarity between the polarisation states present in a field regardless of the presence of temporal fluctuations. Given that the i^{th} and j^{th} patches of the field are normalised, it follows that $0 \leq P^s \leq 1$, where $P^s = 1$ and $P^s = 0$ correspond to fully spatially polarised and spatially unpolarised fields, respectively.

In the case of a field absent of unpolarised part, i.e. fully temporally polarised, Eq. (10) is equivalent to

$$P_{(i,j)}^s = \frac{|\text{Tr}[\Gamma_{(i,j)}]|^2}{\text{Tr}[\Gamma_i] \text{Tr}[\Gamma_j]},$$

or, in more conventional notation, to

$$P^s(\mathbf{r}_i, \mathbf{r}_j, 0) = \frac{|\text{Tr}[\Gamma(\mathbf{r}_i, \mathbf{r}_j, 0)]|^2}{\text{Tr}[\Gamma(\mathbf{r}_i, \mathbf{r}_i, 0)] \text{Tr}[\Gamma(\mathbf{r}_j, \mathbf{r}_j, 0)]}. \quad (11)$$

Given in addition that $\text{Tr}[\Gamma(\mathbf{r}_i, \mathbf{r}_j, \tau)] = \langle \vec{\mathbf{E}}^\dagger(\mathbf{r}_i, t) \cdot \vec{\mathbf{E}}(\mathbf{r}_j, t - \tau) \rangle$ for this particular case, one can also write

$$P^s(\mathbf{r}_i, \mathbf{r}_j, 0) = \frac{\langle \vec{\mathbf{E}}^\dagger(\mathbf{r}_i, t) \cdot \vec{\mathbf{E}}(\mathbf{r}_j, t) \rangle^2}{\langle \vec{\mathbf{E}}(\mathbf{r}_i, t) \rangle^2 \langle \vec{\mathbf{E}}(\mathbf{r}_j, t) \rangle^2} = \cos^2 \theta_{(i,j)}, \quad (12)$$

where $\theta_{(i,j)}$ is the angle in Hilbert space, which is related to the orthogonality between polarisation states.

The derivation of the degree of spatial polarisation originated from a two-dimensional scenario; however, Eq. (12) is proof that Eq. (11) can be applied to three-dimensional fields as opposed to existing two-dimensional metrics [16, 17].

4. Degree of temporal polarisation

The degree of temporal polarisation is derived by considering the irradiance described in Eq. (2) when setting $i = j$. This setting, due to the chosen eigensystems, extinguishes the polarised part of the field yielding

$$\text{Tr} [\tilde{\mathbf{G}}_j \Gamma_j \tilde{\mathbf{G}}_j^\dagger] = \text{Tr} [\tilde{\mathbf{G}}_j \Gamma_j^u \tilde{\mathbf{G}}_j^\dagger] \quad (13)$$

at the CCD. By using Eqs. (3) and (4), Eq. (13) can be rewritten as

$$\text{Tr} [\tilde{\mathbf{G}}_j \Gamma_j \tilde{\mathbf{G}}_j^\dagger] = \alpha_j \tilde{\lambda}_j^p (\text{Tr} [\mathbf{I}] - 1) = \frac{\tilde{\lambda}_j^p \text{Tr} [\Gamma_j^u]}{q}, \quad (14)$$

where

$$q = \frac{\text{Tr} [\mathbf{I}]}{\text{Tr} [\mathbf{I}] - 1}.$$

Equation (1) is then written using Eq. (14) and the sum property of the trace as

$$\text{Tr} [\Gamma_j^p] = \text{Tr} [\Gamma_j] - \frac{q}{\tilde{\lambda}_j^p} \text{Tr} [\tilde{\mathbf{G}}_j \Gamma_j \tilde{\mathbf{G}}_j^\dagger]. \quad (15)$$

Since Eq. (1) can also be written using the constituent eigensystems as $\Gamma_j = \tilde{\mathbf{X}}_j (\Lambda_j^p + \alpha_j \mathbf{I}) \tilde{\mathbf{X}}_j^\dagger$, the eigenvectors of the polarised part of the field are seen to be the same as those of the total field. Consequently, Eq. (15) can be rewritten as

$$\text{Tr} [\Gamma_j^p] = \text{Tr} [\Gamma_j] - \frac{q}{\tilde{\lambda}_j^p} \text{Tr} [\Lambda_j (\tilde{\lambda}_j^p \mathbf{I} - \tilde{\Lambda}_j^p)]. \quad (16)$$

It can then be shown (see Eq. 27 in the Appendix) that the second term in the right hand side of Eq. (16) can be rewritten as

$$\text{Tr} [\Lambda_j (\tilde{\lambda}_j^p \mathbf{I} - \tilde{\Lambda}_j^p)] = \tilde{\lambda}_j^p (\text{Tr} [\Lambda_j] - \lambda_j), \quad (17)$$

where λ_j is the largest eigenvalue of Γ_j .

Equation (17) substituted into Eq. (16) represents the irradiance of the polarised part of the field in terms of the polarisation matrix. It thus follows that [9] the ratio of the resulting equation and the total irradiance ($\text{Tr} [\Gamma_j]$) yields the degree of temporal polarisation:

$$P_n^t(\mathbf{r}_j) = 1 - \frac{q(\text{Tr} [\Gamma_j] - \lambda_j)}{\text{Tr} [\Gamma_j]}, \quad (18)$$

where n denotes the dimensionality of the field. Equation (18) quantifies the temporal random fluctuations in a field regardless of the transverse spatial distribution of the polarisation. Note

that because the eigenvalues and the trace of a matrix are invariant to rotation, P_n^t is thus invariant to rotations of the co-ordinate system.

Equation (18) can be applied to two-dimensional fields in general and to three-dimensional fields when two eigenvalues of Γ_j are equal. For two-dimensional fields Eq. (18) becomes

$$P_2^t(\mathbf{r}_j) = \frac{\lambda_j^p}{\lambda_j^p + 2\alpha_j} = \sqrt{1 - \frac{4\text{Det}\Gamma_j}{(\text{Tr}[\Gamma_j])^2}}, \quad (19)$$

which is equivalent to Eq. (5.14) of Ref. [9], whilst when appropriate to three-dimensional fields it becomes

$$P_3^t(\mathbf{r}_j) = \frac{\lambda_j^p}{\lambda_j^p + 3\alpha_j} = \sqrt{\frac{3\text{Tr}[\Gamma_j^2]}{2(\text{Tr}[\Gamma_j])^2} - \frac{1}{2}}, \quad (20)$$

which is again equivalent to Eq. (18) of Ref. [10]. Applications of Eq. (18) in quantum optics have been discussed before [18].

It can be seen from Eqs. (19) and (20) that $0 \leq P^t(\mathbf{r}_j) \leq 1$ for every j . When the beam is fully temporally polarised α_j equals to zero, and hence $P^t(\mathbf{r}_j)$ equals to one. For a temporally unpolarised beam, λ_j^p equals to zero and consequently $P^t(\mathbf{r}_j)$ equals to zero.

5. Remarks

As a remark note that Eq. (9) represents an irradiance measurement in terms of polarisation matrices; to consider an optical element instead, this equation can be rewritten as

$$I_{(j,j)}^p = \text{Tr}[\tilde{\Phi}_j \Lambda_j] - \text{Tr}[\tilde{\mathbf{J}}_j \Gamma_j], \quad (21)$$

where $\tilde{\mathbf{J}}_j$ is a matrix representing a non-depolarising polarisation optical element, and $\tilde{\Phi}_j$ is a matrix containing in the diagonal the eigenvalues of $\tilde{\mathbf{J}}_j$.

Also note the similarity between Eq. (11) and the degree of spatial coherence given by [9]

$$\mu(\mathbf{r}_i, \mathbf{r}_j, \tau) = \frac{\text{Tr}[\Gamma(\mathbf{r}_i, \mathbf{r}_j, \tau)]}{\sqrt{\text{Tr}[\Gamma(\mathbf{r}_i, \mathbf{r}_i, 0)]} \sqrt{\text{Tr}[\Gamma(\mathbf{r}_j, \mathbf{r}_j, 0)]}}, \quad (22)$$

where τ is a time difference at an observation point resulting from the optical path difference between the points determined by \mathbf{r}_i and \mathbf{r}_j . Squaring Eq. (22), substituting it into Eq. (11) and setting τ equal to zero, one obtains

$$P^s(\mathbf{r}_i, \mathbf{r}_j, 0) = \mu^2(\mathbf{r}_i, \mathbf{r}_j, 0). \quad (23)$$

This equation shows that the DOSP can be measured using the interference pattern produced by a two pinhole interferometer. In the case of measuring an incoherent field, Eq. (23) holds only when the optical paths between the observation point and the pinholes are equal. For coherent fields, this equation holds when the optical path difference is a multiple of the wavelength.

6. Example

To illustrate the DOSP and DOTP, consider the field distribution at the back focal plane of a high NA lens produced by a single molecule. It is assumed that the molecule is on-axis, in focus, fluorescent, its dipole moment is $(1,0,1)/\sqrt{3}$, exhibits circular dichroism, and it can undergo stationary random temporal fluctuations (angular wobble). The analytical form of the field when illuminating the molecule with unpolarised light can thus be written as [19]

$$\vec{\mathbf{E}}(\mathbf{r}, t) = \mathbf{L}(\mathbf{r}) \cdot \left[\frac{1}{|\mathbf{r}|^3} \mathbf{r} \times (\mathbf{r} \times \mathbf{p}'(t)) \right], \quad (24)$$

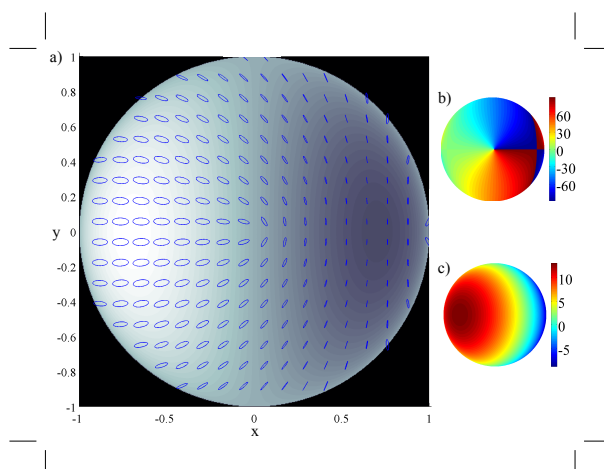


Fig. 2. (a) Polarised part of the field distribution produced by a single molecule whose dipole moment is $(1,0,1)/\sqrt{3}$ and exhibits circular dichroism. The irradiance is represented by the grayscale in positive, and the ellipses depict the polarised part of the field at the given points. Figures (b) and (c) show the distribution of the azimuthal angle and the ellipticity of the polarisation, respectively.

where $\mathbf{L}(\mathbf{r})$ is the generalised Jones matrix of the lens in Cartesian coordinates, and $\mathbf{p}'(t) = \mathbf{p} + \Delta\mathbf{p}(t)$ is the dipole moment \mathbf{p} of the molecule perturbed by a temporal random fluctuation $\Delta\mathbf{p}(t)$.

The field distribution produced by the molecule in the back focal plane of a high NA lens is shown in Fig. 2(a). This distribution is obtained from the polarisation matrix, which is found using Eq. (24). The grayscale represents the irradiance in positive (white equals to bright). The ellipses represent the polarisation state of the field and its magnitude at the given points. These ellipses are plotted using the azimuth angle and ellipticity calculated from the polarisation matrix. Figures 2(b) and 2(c) show the transverse distribution of the field decomposed in azimuth angle and ellipticity, respectively. Note that Fig. 2 can be computed regardless of the degree of temporal polarisation since only the polarised part of the field is needed to be generated.

The DOSP can also be calculated regardless of the DOTP of the beam due to the generality of Eq. (10). The DOSP of such a field distribution is depicted in Fig. 3. Given that Eq. (10) is a function of two sets of spatial co-ordinates, the figure is built from the subfigures corresponding to the coordinates $\mathbf{r}_i = (x_i, y_i, z_i = 0)$ positioned on the coordinates $\mathbf{r}_j = (x_j, y_j, z_j = 0)$. By definition, the point denoted by \mathbf{r}_i in the subfigure equals to one if the subfigure is positioned at $\mathbf{r}_i = \mathbf{r}_j$. The visualisation of the DOSP aims to the localisation of the regions in the field that increase the effect of the spatial variations on the measurement of temporal fluctuations. Quantification of the DOSP leads to the possession of a confidence level.

Consider the examples shown in Fig. 4 to illustrate the influence of the DOSP on the measurement of the DOTP. This figure shows column-wise three examples with different amounts of temporal fluctuations. The case when the molecule is static is shown in the left column, the centre and right columns depict the cases when angular perturbations are added to the position of the molecule; the greatest angular perturbation is shown in the column on the right. The first row depicts the dipole moment of the molecule at specific times. The black dot represents the value of the initial dipole moment in a Cartesian coordinate system, and the red dots represent

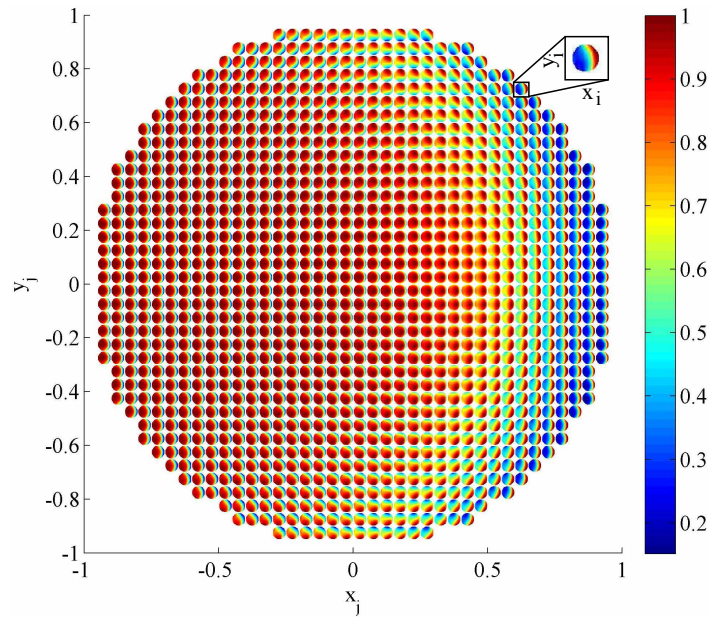


Fig. 3. Degree of spatial polarisation of the field produced by a single molecule at the back focal plane of a high NA lens. The figure consists of subfigures that correspond to the coordinates $\mathbf{r}_i = (x_i, y_i, z_i = 0)$ centred on the coordinates $\mathbf{r}_j = (x_j, y_j, z_j = 0)$.

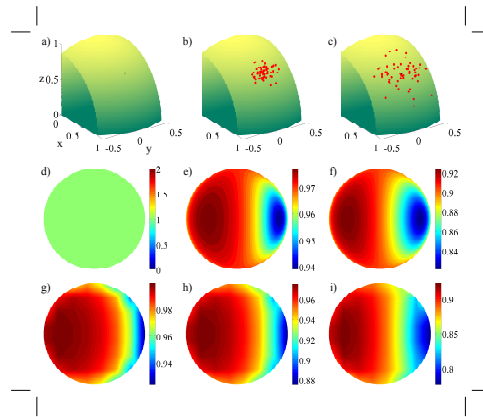


Fig. 4. Effect of angular perturbations on the DOTP when averaging over finite areas. The examples are given column-wise for different amounts of angular perturbation increasing from left to right (left column being the static case). Top row depicts the dipole moment of the molecule at specific times. The black dot represents the initial dipole moment and the red ones depict the subsequent ones. The middle row is the DOTP measuring with a CCD formed of infinitesimally small pixels. Bottom row is the DOTP measured using a CCD whose pixel size is 1/8th of the total area of the beam.

subsequent dipole moments. The second row depicts the DOTP when measured with a CCD having infinitesimally small pixels. Notice that due to the polarisation distribution present in the beam, the DOTP is more susceptible to changes in regions where the field is less homogeneous. The third row is the “measured DOTP” — obtained when averaging the field over pixels of finite size. The size of the pixels is assumed to be one eighth of the total area of the beam, e.g. small beam diameter or low quality camera. For pixels of smaller diameter, the distribution profile of the DOTP remains the same but the range decreases. The results from the static case (left column) shows clearly the effect of the spatial distribution of the field on the DOTP. For a static dipole, the DOTP is expected to be constant as illustrated in Fig. 4(d). Consequently, as shown in Fig. 4(g), a CCD camera of finite pixel size measures erroneously the field as being partially polarised. Note however that if the DOSP and DOTP are measured in the image plane, this fact implies that the polarisation of the field is varying within the diffraction limit of the system.

A confidence level on the measurement of the DOTP can be established using the DOSP to design beams or in measurements if a priori information is present. For example, note the similarity between the measured DOTP (bottom row) and the DOSP (Fig. 3). In the static dipole case, the measured DOTP (Fig. 4g) is closer to unity on the left side of the beam where the DOSP is also close to unity. As the fluctuations of the dipole increase, the distribution of the measured DOTP results from the combination of the DOTP, corresponding to infinitesimal pixel size, and the DOSP. However, the measured DOTP always yields the real value of the DOTP in areas where the DOSP is unity. A confidence level can thus be established using, for example, the mean value of each subfigure in the DOSP. In the case of a beam exhibiting symmetry such as a radially polarised beam, the DOSP inherits the symmetry as shown in Fig. 5. In this case, the contribution of the spatial variations to the DOTP is the same across most of the beam. The only point where the DOSP is different is at the centre point of the beam where the DOSP cannot be defined due to the phase singularity. If a finite-sized pixel is centred at this point, the measured DOTP results as fully unpolarised independently of the size of the pixel. Notice that one can measure the DOSP of a beam using a high-resolution system sacrificing acquisition speed, assess the confidence level, and thus optimise the speed of the system by adjusting the resolution.

7. Conclusion

In summary, we have derived a formula using the polarisation matrix that describes the degree of temporal polarisation in an optical system of arbitrary dimensions. The degree of temporal polarisation, which is rotationally invariant, was shown to reduce to the two- and three-dimensional versions of the well-known degree of polarisation when the dimensions are appropriately restricted. We have also introduced a new metric that describes the degree of spatial polarisation in a field regardless of temporal fluctuations present. This metric enables one to build more realistic models to describe light–matter interactions, such as molecular dynamics or metamaterial characterisation. It is also possible to use this metric to evaluate beams having different spatially inhomogeneous polarisation distributions, such as the much researched donut or singular beams. The formulation for both spatial and temporal degree of polarisation were shown to be consistent with the corresponding quantities defined in optical coherence theory. Finally, examples were given in the context of single molecule detection to illustrate the DOSP and the DOTP when measuring asymmetrically and radially polarised beams.

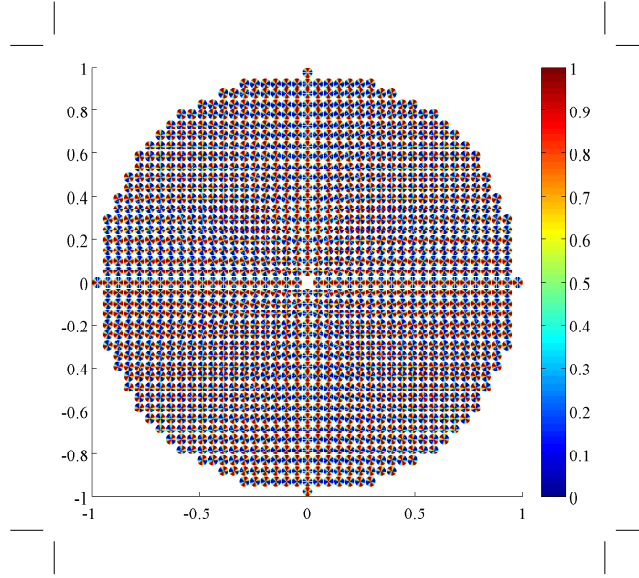


Fig. 5. Degree of spatial polarisation of the field produced by a radially polarised beam. The figure consists of subfigures that correspond to the coordinates $\mathbf{r}_i = (x_i, y_i, z_i = 0)$ centred on the coordinates $\mathbf{r}_j = (x_j, y_j, z_j = 0)$.

8. Appendix

The following is the proof of Eq. (7), which was used to rewrite Eq. (6). Substituting $\Gamma_j = \tilde{\mathbf{X}}_j(\Lambda_j^p + \alpha_j \mathbf{I})\tilde{\mathbf{X}}_j^\dagger$ and $\lambda_j = \lambda_j^p + \alpha_j$ into

$$\text{Tr}[\Gamma_j] - \lambda_j = \alpha_j(\text{Tr}[\mathbf{I}] - 1) \quad (25)$$

yields

$$\text{Tr}[\Lambda_j^p + \alpha_j \mathbf{I}] - \lambda_j^p - \alpha_j = \alpha_j(\text{Tr}[\mathbf{I}] - 1),$$

which can be expanded using the additive property of the trace to obtain

$$\text{Tr}[\Lambda_j^p] + \alpha_j \text{Tr}[\mathbf{I}] - \lambda_j^p - \alpha_j = \alpha_j \text{Tr}[\mathbf{I}] - \alpha_j,$$

and to finally yield

$$\lambda_j^p = \lambda_j^p$$

since $\text{Tr}[\Lambda_j^p] = \lambda_j^p$.

The following is the proof of Eq. (8), which was also used to rewrite Eq. (6). Substituting $\Lambda = \Lambda^p + \alpha \mathbf{I}$ and $\lambda = \lambda^p + \alpha$ into

$$\text{Tr}[\tilde{\Lambda}_i \Lambda_j] - \tilde{\lambda}_i \lambda_j = \tilde{\alpha}_i \alpha_j (\text{Tr}[\mathbf{I}] - 1) \quad (26)$$

and rearranging yields

$$\text{Tr}[(\tilde{\Lambda}_i^p + \tilde{\alpha}_i \mathbf{I})(\Lambda_j^p + \alpha_j \mathbf{I})] = (\tilde{\alpha}_i + \tilde{\lambda}_i^p)(\alpha_j + \lambda_j^p) + \tilde{\alpha}_i \alpha_j (\text{Tr}[\mathbf{I}] - 1),$$

which can then be simplified using the additive property of the trace to obtain

$$\text{Tr} [\tilde{\Lambda}_i^p \Lambda_j^p] + \tilde{\alpha}_i \text{Tr} [\Lambda_j^p] = -\alpha_j \text{Tr} [\tilde{\Lambda}_i^p] + \tilde{\lambda}_i^p \lambda_j^p + \alpha_j \tilde{\lambda}_i^p + \tilde{\alpha}_i \lambda_j^p$$

and to finally yield

$$\tilde{\lambda}_i^p \lambda_j^p = \tilde{\lambda}_i^p \lambda_j^p$$

since $\text{Tr} [\Lambda_j^p] = \lambda_j^p$.

The following is proof of the equivalence claimed in Eq. (16). Substituting $\Lambda = \Lambda^p + \alpha \mathbf{I}$ into the right hand side of

$$\text{Tr} [\Lambda_j (\tilde{\lambda}_j^p \mathbf{I} - \tilde{\Lambda}_j^p)] = \tilde{\lambda}_j^p (\text{Tr} [\Lambda_j] - \lambda_j) \quad (27)$$

and using the additive property of the trace on the left hand side yields

$$\tilde{\lambda}_j^p \text{Tr} [\Lambda_j] - \text{Tr} [\Lambda_j \tilde{\Lambda}_j^p] = \tilde{\lambda}_j^p (\lambda_j^p + 2\alpha_j - (\lambda_j^p - \alpha_j)),$$

which can be simplified by algebraic manipulation after substituting $\Lambda = \Lambda^p + \alpha \mathbf{I}$ in the left hand side to obtain

$$\begin{aligned} \tilde{\lambda}_j^p (\lambda_j^p + 2\alpha_j) - \tilde{\lambda}_j^p (\lambda_j^p + \alpha_j) &= \tilde{\lambda}_j^p \alpha_j \\ \tilde{\lambda}_j^p \alpha_j &= \tilde{\lambda}_j^p \alpha_j. \end{aligned}$$

Acknowledgments

This research was supported by the Consejo Nacional de Ciencia y Tecnología, the European project no. FP7-ICT-2007-2-224226, and the PhD-PLUS fellowship granted by the Engineering and Physical Sciences Research Council.